Plant Physiology and Biochemistry 65 (2013) 67–74

Contents lists available at SciVerse ScienceDirect

Plant Physiology and Biochemistry

journal homepage: www.elsevier.com/locate/plaphy

Research article

Hydrogen sulfide alleviates cadmium toxicity through regulations of cadmium transport across the plasma and vacuolar membranes in *Populus euphratica* cells

Jian Sun [a], Ruigang Wang [b], Xuan Zhang [c], Yicheng Yu [a], Rui Zhao [c], Zongyun Li [a], Shaoliang Chen [c,*]

[a] College of Life Science, Jiangsu Normal University, Xuzhou 221116, Jiangsu Province, PR China
[b] Center for Research in Ecotoxicology and Environmental Remediation, Agro-Environmental Protection Institute, Ministry of Agriculture, Tianjin 300191, PR China
[c] College of Biological Sciences and Technology (Box 162), Beijing Forestry University, Beijing 100083, PR China

ARTICLE INFO

Article history:
Received 28 November 2012
Accepted 4 January 2013
Available online 28 January 2013

Keywords:
H_2S
Cd flux
Poplar
Antioxidant enzymes
H_2O_2
Intact vacuole
SIET

ABSTRACT

Hydrogen sulfide (H_2S) is emerging as a novel signalling molecule involved in plant growth and responses against abiotic stresses. However, little information is known about its role in cadmium (Cd) detoxification. In the present study, the effects of H_2S on Cd toxicity were investigated in *Populus euphratica* cells using fluorescence imaging technique and a non-invasive vibrating ion-selective microelectrode. Pretreatment with a H_2S donor, sodium hydrosulfide (NaHS), significantly mitigated the Cd-induced programmed cell death in *P. euphratica* cells. The alleviation effect of NaHS was more pronounced at 50–100 μM as compared to low (25 μM) and high doses (200 μM). Under Cd stress, total activities of antioxidant enzymes, such as ascorbate peroxidase, catalase and glutathione reductase, were significantly enhanced in NaHS-treated cells, leading to a decline of H_2O_2 accumulation and lipid peroxidation. Moreover, NaHS reduced Cd accumulation in the cytoplasm but increased the fraction of Cd in the vacuole. Cd flux profiles revealed that H_2S inhibited the Cd influx through the plasma membrane (PM) calcium channels that activated by H_2O_2. NaHS enhanced Cd influx into the vacuole, and the Cd influx was dependent on the pH gradients across the tonoplast. Taken together, these results suggest that H_2S alleviates Cd toxicity via the improvement of antioxidant system and cellular Cd homeostasis. The up-regulation of antioxidant enzymes by H_2S reduced the accumulation of H_2O_2, and thus decreased Cd influx through the H_2O_2-activated PM calcium channels. The H_2S-simulated vacuolar Cd sequestration was presumably due to the activation of tonoplast Cd^{2+}/H^+ antiporters.

1. Introduction

Cadmium (Cd), one of the most toxic heavy metals for plants, has a strong inhibitory effect on plant growth and development [1]. Cd ions enter plant cells through ZIP (Zinc-regulated transporter/Iron-regulated transporter-like protein) transporters and non-selective cation channels (NSCC) [2]. The uptake and accumulation of Cd in the cytoplasm usually causes reactive oxygen species (ROS) burst by displacing Fe from proteins and inhibiting the electron transport chain in the chloroplast and mitochondria, as well as by inhibiting antioxidative systems in plant cells [3,4]. The generation of excess ROS reacts with lipids, proteins and pigments, and finally results in membrane damage and enzyme inactivation [4]. To avoid the Cd toxicity in the cytoplasm, plant cells compartmentize excess Cd in the vacuoles, cell walls and other organelles [5]. The central vacuoles are primary storage sites for Cd in most plant species [6]. Cd is often sequestered in the vacuole as Cd–phytochelatin complexes, which is mediated by ABC transporters, such as orthologues of AtMRP3 [7]. In addition, Cd can also be transported across the tonoplast by Cd^{2+}/H^+ antiporters, such as orthologues of AtCAX2 and AtCAX4 [8,9], or by heavy metal P_{1B}-ATPases, e.g. orthologues of AtHMA3 [10].

Using priming techniques (e.g., external application of natural or synthetic compounds in plants) to facilitate plant acclimation to environmental stresses has received much attention in recent years [11]. Exogenous supplement of chemicals, such as calcium, proline, glycinebetaine and nitric oxide (NO), was able to alleviate Cd toxicity in various species [12–16]. Pretreatment with selenium, proline and glycinebetaine in Cd-stressed rapeseed seedlings and tobacco BY-2 cells reduced the oxidative damage by recovering the antioxidant defence system [12,13]. Exogenous NO enhanced Cd tolerance by increasing pectin and hemicellulose contents in the cell wall of rice roots [14]. High concentration of external calcium

* Corresponding author. Tel.: +86 10 62338129; fax: +86 10 62336164.
E-mail address: Lschen@bjfu.edu.cn (S. Chen).

0981-9428/$ – see front matter © 2013 Elsevier Masson SAS. All rights reserved.
http://dx.doi.org/10.1016/j.plaphy.2013.01.003

inhibited Cd uptake and translocation to the shoot in *Sedum alfredii* [15]. Furthermore, exogenously applied sulphur rescued Cd-induced inhibition of photosynthetic capacity in mustard [16].

Hydrogen sulfide (H_2S), a critical signal molecule in animals, is indispensable for a variety of physiological functions, such as anti-inflammatory and blood pressure regulation [17]. Recent studies in plants revealed that H_2S plays multiple roles in various physiological processes, e.g., adventitious root and lateral root formation [18], stomatal movement [19], photosynthesis and abiotic stress responses [20–22]. In *Arabidopsis*, H_2S fumigation and H_2S donor treatment stimulated the expression of drought-associated genes that contributing to drought resistance [21]. In addition, H_2S improved salt tolerance via regulating K^+/Na^+ homeostasis and antioxidant system in *Medicago sativa* seedlings [22]. Interestingly, H_2S functions as a potent antioxidant in plants upon heavy metal stresses by enhancing the transcripts and/or activities of antioxidant enzymes [23]. Li et al. [24] reported that H_2S alleviated Cd toxicity through recovering the NO-dependent antioxidant defence system in the roots of alfalfa seedlings. However, the mechanisms for H_2S alleviation of Cd toxicity are largely unknown in woody plants.

The genus *Populus* consists of five sections with about 30–40 species occurring worldwide [25]. *Populus* species are usually considered as Cd-tolerant even different clones of the same poplar species exhibits variable Cd tolerance due to intraspecific genetic dissimilarity [26]. *Populus euphratica* is salt-resistant [27–31] but sensitive to Cd [32]. The higher Cd susceptibility of *P. euphratica* is due to the failure to activate early protective responses upon Cd exposure, compared to *Populus* × *canescens* [32]. Therefore, *P. euphratica* is an ideal material to explore the effects of exogenous chemicals on Cd detoxification in woody plants. The aim of this work is to investigate the potential mechanisms required for the H_2S-induced alleviation of cellular Cd toxicity in poplar species. Cell culture of *P. euphratica* is a model system to examine ROS and ionic homeostasis because of cellular homogeneity and undifferentiated state [28,29]. In this study, we clarified the H_2S induction of antioxidant enzymes in Cd-stressed *P. euphratica* cells. Using uniform callus cells and vacuoles, effects of H_2O_2, pH, NaHS, catalase, and calcium channel inhibitor on Cd fluxes were also examined in this study.

2. Results

Cd stress causes Cd toxicity in plant cells, leading to programmed cell death (PCD) [33]. In this study, Cd-induced cell death was examined in a woody species, *P. euphratica*. Treatment with 100 μM $CdCl_2$ for 72 h resulted in a significant reduction of cell viability in *P. euphratica* cells (Fig. 1). It is noteworthy that Cd-treated cells displayed several hallmark features of PCD: a clear retraction of the cytoplasm from the cell wall accompanied by shrinkage of the cytoplasm, DNA fragmentation (TUNEL positive nuclei) and condensed or stretched chromatin (Hoechst 33342 positive nuclei; Fig. 1). NaHS, a H_2S donor, was able to alleviate the Cd toxicity in *P. euphratica* cells (Table 1). We found that the alleviation effect of NaHS was more pronounced at 50–100 μM as compared to low (25 μM) and high doses (200 μM; Table 1). Pretreatment with the same concentration of Na_2SO_4 had no effect on Cd-induced PCD in *P. euphratica* cells (data not shown), suggesting that the effect of NaHS on Cd detoxification was due to H_2S. We adopted a working concentration of 50 μM in further experiments, which reduced Cd-stimulated PCD in *P. euphratica* cells but had no inhibitory effect on cell viability over the observation time (Table 1).

In general, Cd toxicity was attributed to the formation of reaction oxygen species (ROS) and/or reduced antioxidant capacity in plants [3,4]. Therefore, we measured activity of antioxidant enzymes, lipid peroxidation and H_2O_2 accumulation in Cd-stressed *P. euphratica* cells. Cd treatment (100 μM) resulted in a significant reduction of antioxidant enzymes in *P. euphratica* cells, up to 31% (glutathione reductase, GR), 37% (catalase, CAT) and 49% (ascorbate peroxidase, APX; Fig. 2A–C). However, treatment with 50 μM NaHS reduced the Cd inhibition of these enzymes (Fig. 2A–C). In the absence of Cd stress, incubation of poplar cells with NaHS had no significant effect on activity of antioxidant enzymes (Fig. 2A–C). We used a specific H_2O_2 probe, H_2DCF-DA, to visualize H_2O_2 in *P. euphratica* cells. A 72-h exposure to $CdCl_2$ (100 μM) resulted in a significant rise of H_2DCF-dependent fluorescence, indicating a H_2O_2 burst in *P. euphratica* cells (Fig. 2E). However, the Cd-induced production of H_2O_2 was drastically decreased by NaHS treatment (Fig. 2E). In accordance, NaHS significantly reduced MDA content in Cd-treated cells, suggesting that the Cd-stimulated lipid peroxidation was lowered by NaHS (Fig. 2D).

Vacuolar compartmentation of Cd is of importance for plant cells to avoid Cd toxicity [5,6]. In this study, we measured Cd distribution with a Cd-sensitive fluorescent probe, Leadmium™ Green. *P. euphratica* cells exhibited a marked increase in Leadmium™ Green-specific

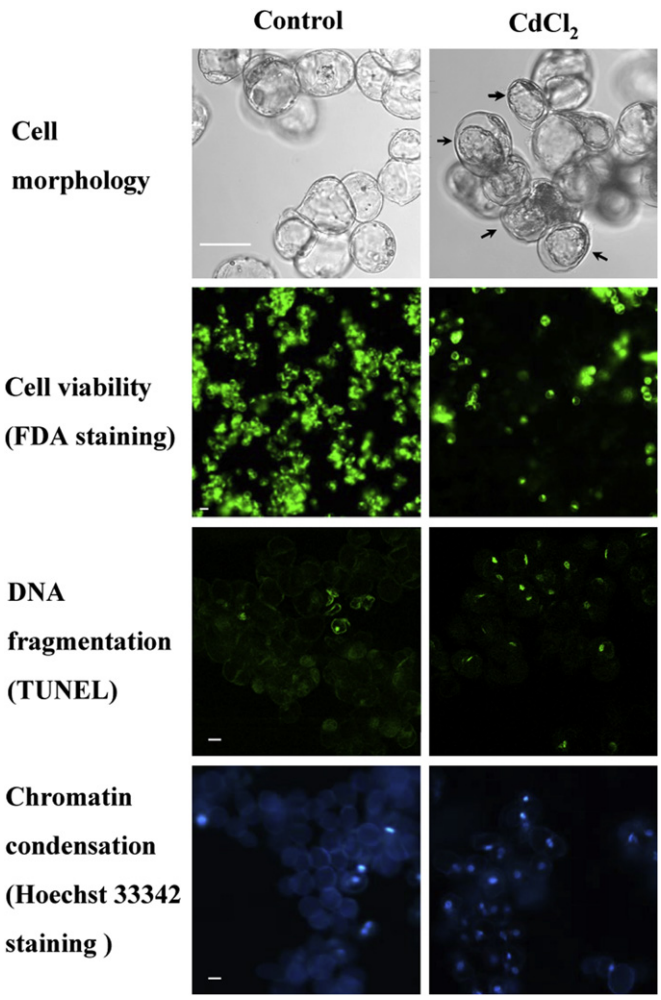

Fig. 1. Cadmium (Cd) induced programmed cell death (PCD) in *Populus euphratica* cells. Representative images depict the effects of Cd stress (100 μM, 72 h) on cell morphology (arrows highlight retraction of cytosol from cell wall), viability (fluorescein diacetate [FDA, green] denotes live cells), DNA fragmentation (TUNEL staining, green fluorescein isothiocyanate indicates an increase in DNA fragmentation), chromatin condensation (Hoechst 33342, blue). Images were taken after 72 h of incubation in 100 μM $CdCl_2$. Scale bars, 50 μm. (For interpretation of the references to colour in this figure legend, the reader is referred to the web version of this article.)

Table 1
Concentration effects of NaHS (0–200 μM) on cell viability (FDA staining), DNA fragmentation (TUNEL analysis), and chromatin condensation (Hoechst 33342 staining) in the presence and absence of 100 μM $CdCl_2$ (72 h) in *Populus euphratica* cells. Values (±standard deviation) represent the mean of 200 cells quantified from three biologically independent samples. Values labelled with different letters (a, b, c, d) in the same row are significantly differed at $P < 0.05$.

	NaHS (0 μM)		NaHS (25 μM)		NaHS (50 μM)		NaHS (100 μM)		NaHS (200 μM)	
	−Cd	+Cd	−Cd	+Cd	−Cd	+Cd	−Cd	+Cd	−Cd	+Cd
Cell viability (%)	94 ± 3a	42 ± 7d	91 ± 5a	56 ± 8c	90 ± 3a	75 ± 6b	88 ± 5a	66 ± 8bc	83 ± 4ab	40 ± 8d
DNA fragmentation (%)	5 ± 2c	43 ± 5a	6 ± 3c	34 ± 5a	8 ± 2c	18 ± 4b	10 ± 3c	25 ± 4b	22 ± 4b	42 ± 6a
Chromatin condensation (%)	8 ± 3d	48 ± 7a	9 ± 2d	42 ± 4a	9 ± 2d	20 ± 5c	12 ± 4d	31 ± 3b	21 ± 5c	50 ± 6a

fluorescence after 72 h of Cd stress, but Cd-specific fluorescence was nearly undetectable in control cells (Fig. 3A). Of note, more of the Cd-specific fluorescence was distributed in the cytoplasmic region than in the vacuole (Fig. 3). However, the pattern of Cd partitioning within cells was altered by the application of NaHS. NaHS drastically reduced the fraction of Cd partitioned to the cytoplasm (the Leadmium™ Green-specific fluorescence decreased by 40%), which was parallelled with increases in the fraction of Cd partitioned to the vacuole (the Leadmium™ Green-specific fluorescence increased by 48%; Fig. 3). Treatment NaHS alone had no effect on cellular Cd fluorescence compared with control cells (Fig. 3).

In order to explore the NaHS-induced alterations of cellular Cd distribution, we measured steady-state Cd fluxes across the plasma and vacuolar membranes in Cd-stressed *P. euphratica* cells. After exposure to Cd stress for 24–72 h, *P. euphratica* cells exhibited a steady Cd influx, ranging from 6.4 to 9.3 pmol cm^{-2} s^{-1} (Fig. 4A). However, application of NaHS significantly decreased the Cd influx by 44–53% at three time points measured (24, 48, and 72 h; Fig. 4A). Application of a H_2O_2 scavenger, CAT, resulted in a trend similar to that of NaHS (Fig. 4A). To examine Cd transport across the tonoplast, we isolated intact vacuoles from Cd-stressed *P. euphratica* cells for flux recording. Our SIET data showed that *P. euphratica* vacuoles also exhibited a steady Cd influx and the mean flux rate was 0.8 pmol cm^{-2} s^{-1} (Fig. 4B). Interestingly, NaHS significantly enhanced the Cd influx in Cd-treated vacuoles, reaching 1.4–1.7 pmol cm^{-2} s^{-1} (Fig. 4B). Our results showed that H_2S mediated

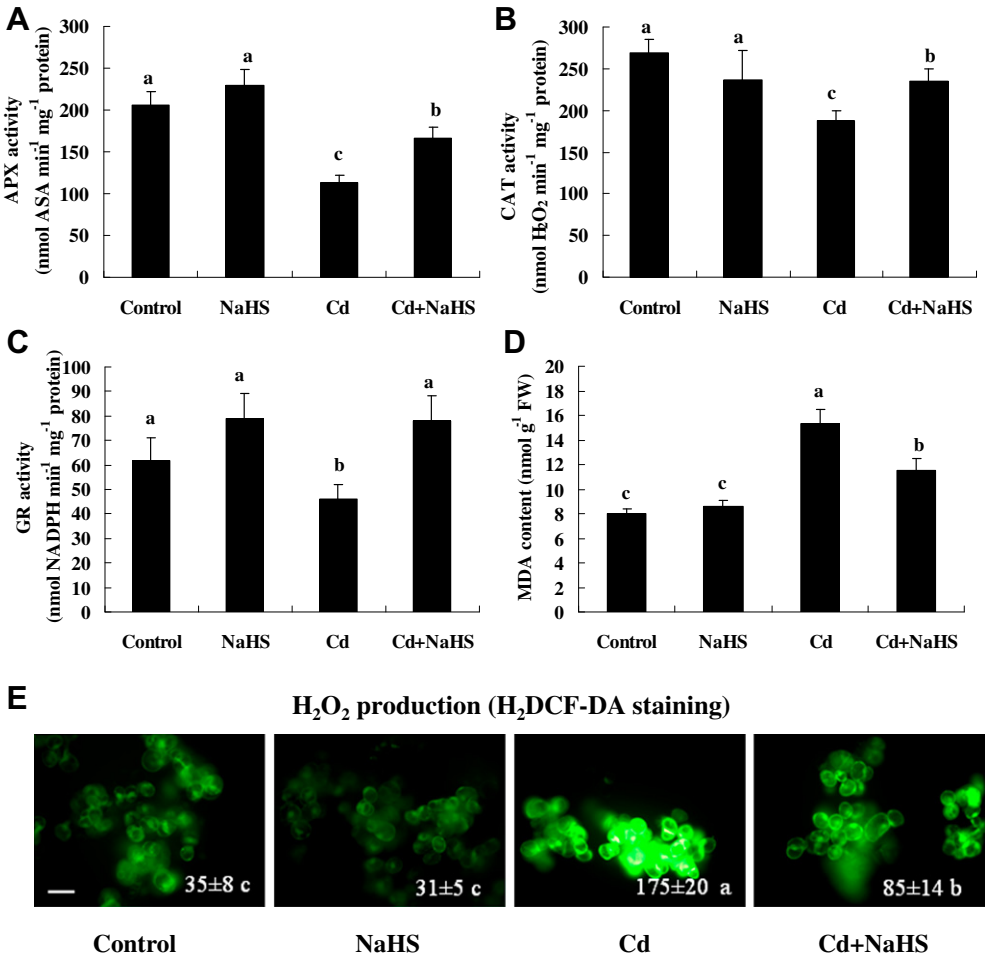

Fig. 2. Effects of NaHS on activities of antioxidant enzymes, lipid peroxidation and H_2O_2 accumulation in $CdCl_2$-treated *Populus euphratica* cells. *P. euphratica* cells were treated with $CdCl_2$ (100 μM) for 72 h in the presence and absence of NaHS (50 μM). (A–C) Activity of ascorbate peroxidase (APX), catalase (CAT), and glutathione reductase (GR). (D) MDA content. Each column is the mean of three biologically independent samples and bars represent the standard error of the mean. Columns labelled with different letters (a, b, c) are significantly different at $P < 0.05$. (E) Representative images showing H_2O_2 accumulation (H_2DCF-DA fluorescence, green). Scale bars, 100 μm. Insert values (±standard deviation) represent mean fluorescence of 200–250 cells quantified from three biologically independent samples. Values labelled with different letters (a, b, c) are significantly different at $P < 0.01$. (For interpretation of the references to colour in this figure legend, the reader is referred to the web version of this article.)

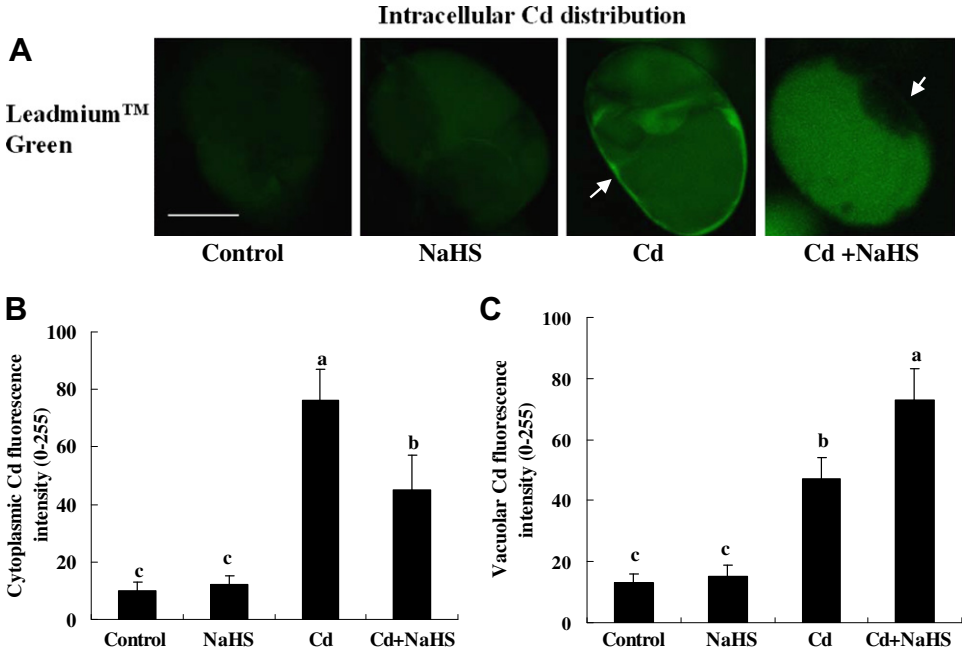

Fig. 3. Effects of NaHS on Cd subcellular distribution in Cd-stressed *Populus euphratica* cells. *P. euphratica* cells were treated with $CdCl_2$ (100 μM) for 72 h in the presence and absence of NaHS (50 μM). (A) Representative images depict the Cd subcellular distribution (indicated by the Cd-sensitive fluorescent probe, Leadmium™ Green). Arrows indicate cytoplasmic Cd accumulation in *P. euphratica* cells. Scale bar, 25 μm (B, C) Cd levels within the cytoplasm (B) and vacuole (C). Columns represent the means of at least 100 individual cells quantified from three biologically independent samples. Whiskers represent the standard error of the mean. Different letters (a, b, c) denote significant differences between treatments ($P < 0.05$). (For interpretation of the references to colour in this figure legend, the reader is referred to the web version of this article.)

the entry and sequestration of Cd into *P. euphratica* vacuoles. In contrast to NaHS, CAT had no effect on vacuolar Cd flux under Cd stress (Fig. 4B).

The effects of H_2O_2, pH, and Ca^{2+} channel inhibitors on transient Cd flux were also characterized in this study. Addition of 10 μM $CdCl_2$ induced a Cd influx through the PM with a mean rate of 2.9 pmol cm^{-2} s^{-1} (Fig. 5A, C). It is noting that the Cd influx was significantly enhanced after exposure to 3 mM H_2O_2 (Fig. 5A, C). However, the H_2O_2-stimulated entry of Cd was inhibited by $LaCl_3$, a PM calcium channel inhibitor (Fig. 5A, C). Our results suggest that the Cd influx is likely via calcium channels in the PM [34]. Addition of 10 μM $CdCl_2$ to intact vacuoles (the pH of measuring solution is 7.2) induced a transient Cd influx across the tonoplast with a mean rate of 0.5 pmol cm^{-2} s^{-1} (Fig. 5B, D). Interestingly, we found that the vacuolar Cd influx was absent when the measuring solution was changed to an acidic environment (pH 5.5; Fig. 5B, D), suggesting that the vacuolar Cd flux was dependent on the pH gradient across the tonoplast. We found that the entry of Cd into vacuole was not altered by H_2O_2, irrespective of external pH values, 5.5 or 7.2 (Fig. 5B, D), indicating that the vacuolar Cd flux is independent of H_2O_2.

3. Discussion

Cd uptake and accumulation in plants usually reduces growth and even causes cell death [3,4]. In this study, Cd-treated *P. euphratica* cells exhibited a clear shrinkage of the cytoplasm, indicating disturbance of the water balance. This is similar to the finding of Polle et al. [32], who found that *P. euphratica* leaves displayed water loss and wilting under Cd stress [32]. Moreover, Cd treatment induced a loss of cell viability accompanied with DNA fragmentation and chromatin condensation in this Cd-susceptible poplar (Fig. 1). This was consistent with other reports that Cd caused occurrence of PCD in various plant systems [33]. Of note, we found that the Cd-induced PCD in the poplar was alleviated by a H_2S donor, NaHS (Table 1). Similarly, Li et al. reported that NaHS mitigated syndromes associated with Cd toxicity in herbaceous plant [24]. Activity of antioxidant enzymes was usually up-regulated in Cd-stressed plants, because an activated antioxidant system is beneficial to scavenge ROS and thus inhibits subsequent detrimental effects that induced by excess ROS [2–4,24]. In this study, a significantly increased H_2O_2 was observed in Cd-stressed *P. euphratica* cells (Fig. 2). The H_2O_2 burst may contribute to the occurrence of PCD, as H_2O_2 burst is the most important signal involved in Cd-induced cell death in plants [2–4,24]. It has repeatedly shown that H_2S functions as a modulator of antioxidant system in various animal and plant species [17,22–24]. In *M. sativa* roots, the beneficial effects of H_2S on Cd toxicity have been ascribed to the up-regulation of antioxidant enzymes [24]. In this study, we found that NaHS rescued the Cd-induced inhibition of antioxidant enzymes, and thus down-regulated the H_2O_2 level in *P. euphratica* cells (Fig. 2). As a result, Cd-stimulated lipid peroxidation was reduced in long term-stressed *P. euphratica* cells (Fig. 2).

Restricting entry of Cd is critical for plant cells to cope with Cd environments. It has shown that Cd sensitivity of *P. euphratica* is due to its higher uptake and transport rate of Cd to aboveground tissues, compared to *P.* × *canescens* [32]. In this study, *P. euphratica* cells also exhibited a marked Cd accumulation, especially in the cytoplasmic region (Fig. 3). We observed that NaHS treatment decreased Cd accumulation in the cytoplasm (Fig. 3). This agrees with the result of Li et al. [24], who discovered that NaHS pre-treatment decreased Cd content in Cd-treated *M. sativa* roots. Moreover, flux profiles showed that NaHS decreased Cd influx across the PM during a long-term experiment (24–72 h; Fig. 4). Perfus-Barbeoch et al. suggest that the Cd influx into cytosol is mediated by the PM calcium channels in *Arabidopsis* [34]. Similarly, we found that $LaCl_3$, a PM calcium channels inhibitor, significantly inhibited the transient Cd fluxes across the PM in *P. euphratica* cells (Fig. 5). This indicates the involvement of PM calcium channels in the Cd influx. Taken together, H_2S may exert an inhibitory effect on

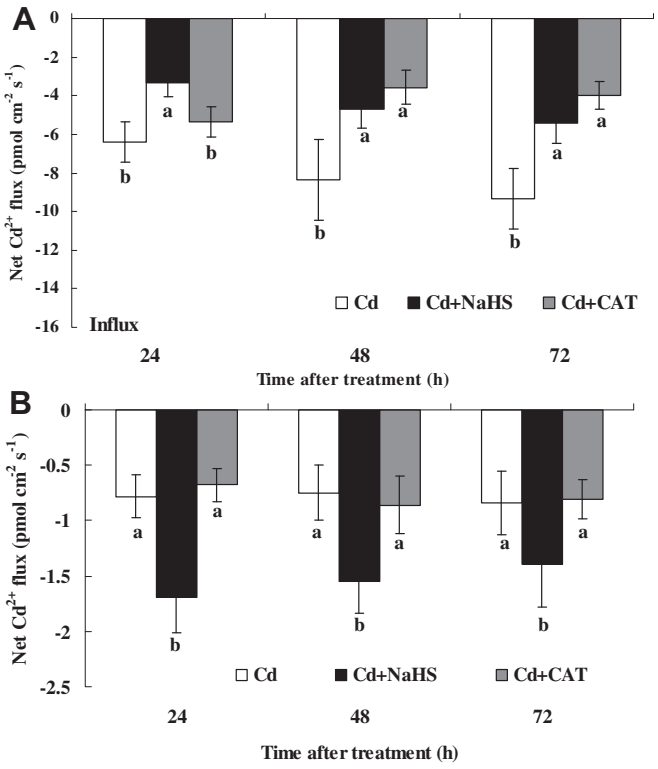

Fig. 4. Effects of NaHS and CAT on steady state Cd fluxes across the plasma and vacuolar membranes in *Populus euphratica* cells. (A) Cd flux across the plasma membrane. *P. euphratica* cells were treated with 100 μM $CdCl_2$ for 24, 48 and 72 h, respectively, in the presence and absence of NaHS (50 μM) or catalase (CAT, 2000 U ml^{-1}). Steady-state Cd fluxes across the PM were recorded in a measuring solution containing 10 μM Cd. (B) Cd flux across the vacuolar membrane. After Cd, NaHS, and CAT treatments as described in (A), protoplasts were isolated and exposed to a sudden hypotonic shock to release intact vacuoles. Steady-state Cd fluxes across the tonoplast were recorded in a measuring solution containing 10 μM Cd. Bars represent the mean of 14–18 individual cells or intact vacuoles quantified from three biologically independent samples and whiskers represent the standard error of the mean. Different letters (a, b) denote significant differences between treatments ($P < 0.05$).

PM calcium channels, thus contributing to the reduction of Cd influx in *P. euphratica* cells. Transient kinetics showed that H_2O_2 accelerated the influx of Cd in *P. euphratica* cells, which was inhibited by the PM calcium channel inhibitor (Fig. 5). This suggests that H_2O_2 activated PM calcium channel and allowed the entry of Cd, as H_2O_2 can activate PM calcium channels in *P. euphratica* callus and *Arabidopsis thaliana* roots [28,35]. In accordance, application of a H_2O_2 scavenger, CAT, lowered the Cd influx across the PM in Cd-stressed *P. euphratica* cells (Fig. 4). Therefore, we speculated that H_2S up-regulated antioxidant enzymes and thus efficiently scavenged H_2O_2 under Cd stress; this led to a decreased Cd influx through the PM calcium channels that activated by H_2O_2.

In addition to restricting the entry of Cd, compartmentizing Cd into vacuoles is a main strategy to maintain a low cytoplasmic Cd in plant cells [2,3]. Hyperaccumulator ecotypes of *S. alfredii* accumulated more Cd in leaf vacuoles than in other intracellular regions [5]. After exposure to Cd stress, Cd was mostly located in the cytoplasm of *Arabidopsis* mutants (hypersensitive phenotype) whereas wild-type *Arabidopsis* plants accumulated more Cd in the vacuole [36]. In this study, we observed that NaHS treatment increased vacuolar fraction of Cd (Fig. 3), suggesting that H_2S stimulated Cd compartmentation into the vacuole. It has shown that Cd transported across the tonoplast via ABC transporters in the form of the Cd–phytochelatin complexes, or by Cd^{2+}/H^+ antiporters and heavy metal P_{1B}-ATPases in plants [7–10]. Our SIET data revealed that H_2S stimulated the influx of free Cd into *P. euphratica* vacuoles (Fig. 4). Moreover, transient kinetics showed that the Cd flux across tonoplast was pH gradient-dependent (Fig. 5). These results imply that H_2S-stimulated Cd influx is partially mediated by the Cd^{2+}/H^+ antiporters in the vacuolar membrane. However, at present, we cannot exclude the possibility that other transport systems were involved in this process. Interestingly, H_2O_2 and CAT treatment did not alter the Cd fluxes (transient and steady state) across the tonoplast (Figs. 4, 5). This suggests that the vacuolar Cd influx in *P. euphratica* cells was independent of H_2O_2.

In conclusion, we discovered that H_2S attenuated Cd toxicity in *P. euphratica* cells by (1) up-regulating activity of antioxidant enzymes, (2) reducing Cd entry into the cytoplasm, and (3) increasing Cd sequestration into the vacuole. Moreover, the up-regulation of antioxidant enzymes by H_2S reduced the accumulation of H_2O_2, and thus decreased Cd influx through the H_2O_2-activated PM calcium channels. The H_2S-simulated vacuolar Cd sequestration was, at least partially, due to the activation of tonoplast Cd^{2+}/H^+ antiporters.

4. Materials and methods

4.1. Plant materials and treatments

Cell cultures of *P. euphratica* Oliver were prepared as described previously [28,29,37]. In brief, callus cells were grown in a Murashige and Skoog (MS) solid medium (2.5% sucrose, pH 5.7), supplemented with 0.25 mg L^{-1} benzyladenine (BA) and 0.50 mg L^{-1} α-naphthaleneacetic acid (NAA), and raised in the dark at 25 °C. Callus cells were subcultured every 15 days, and all experiments were performed at 10 days after cells were transferred to fresh propagation medium. Prior to experimental treatments, cell cultures were suspended in liquid MS (LMS) medium in a superclean bench. Then required amount of stock solution was added to the LMS reaching a final concentration, 100 μM $CdCl_2$. For NaHS treatment, cells were pretreated with 25–200 μM NaHS for 6 h prior to the addition of $CdCl_2$ solution. Thereafter, the cell cultures were raised in the dark at 25 °C for 72 h. Cells treated without NaHS or $CdCl_2$ were used as the control.

4.2. Determination of cell viability

Cell viability was measured with a fluorescein diacetate stain (FDA; Sigma–Aldrich), as described previously [29,37]. In brief, cell suspensions were stained with 20 μg mL^{-1} FDA (Sigma–Aldrich) and then incubated in the dark for 10 min at room temperature. Samples were observed under a Leica inverted fluorescence microscope (Leica Microsystems GmbH, Wetzlar, Germany) at the excitation wavelength of blue light. Cell viability was calculated by counting 8–10 randomly selected fields and for each, at least 300 cells were measured.

4.3. In situ detection of DNA fragmentation

Terminal deoxynucleotidyl transferase-mediated dUTP nick end labelling (TUNEL) was used to visualize cells with fragmented DNA [37]. Cells were collected on the poly-L-lysine-pretreated cover slips (2 × 2 cm), washed in phosphate-buffered saline (PBS, pH 7.2) for 5 min, fixed in 4% (w/v) paraformaldehyde in PBS for 20 min prior to a final wash with PBS. In situ nick end labelling of fragmented nuclear DNA was performed in a humid chamber for 1 h in the dark at 37 °C with the DeadEnd Fluorometric TUNEL system (Promega). The labelling reaction was stopped with 2× SSC (kit supplied) and the slides were rinsed with PBS three times. The fluorescence was visualized under a Leica SP5 confocal microscopy with an excitation

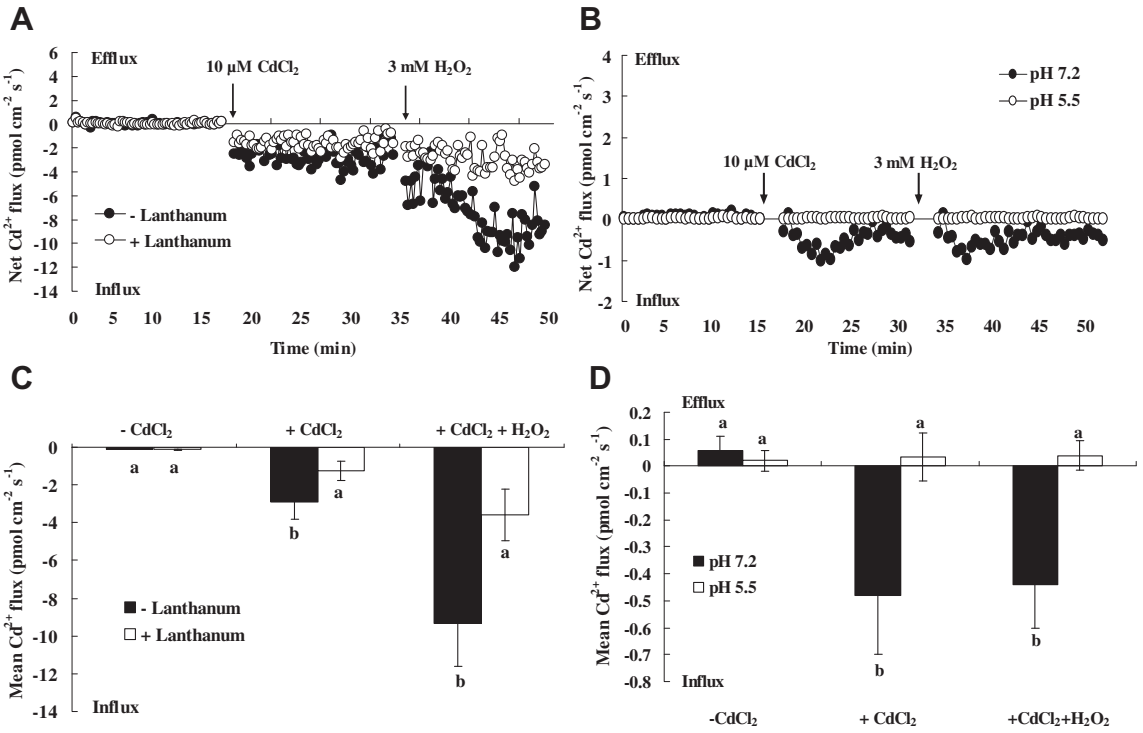

Fig. 5. Effects of H_2O_2, PM calcium channel inhibitor, and pH on transient Cd flux across the plasma and vacuolar membranes in *P. euphratica* cells. (A) Transient Cd flux across the plasma membrane in response to $CdCl_2$ (10 μM) and H_2O_2 (3 mM) in the presence and absence of PM calcium channel inhibitor, $LaCl_3$ (5 mM). Each point represents the mean of six individual cells. (B) Transient Cd flux across the vacuolar membrane in response to $CdCl_2$ (10 μM) and H_2O_2 (3 mM). Protoplasts were isolated from control cells and exposed to a sudden hypotonic shock to release intact vacuoles. Then transient Cd fluxes across the tonoplast were recorded in measuring solutions with pH 5.5 or 7.2. Each point represents the mean of six intact vacuoles. (C, D) Mean values for transient Cd fluxes before (−) and after (+) the addition of $CdCl_2$ and H_2O_2. Bars represent the mean of six individual cells or intact vacuoles quantified from three biologically independent samples and whiskers represent the standard error of the mean. Different letters (a, b) denote significant differences between treatments ($P < 0.05$).

wavelength of 488 nm and an emission wavelength of 515 nm for fluorescein isothiocyanate (FITC). A negative control was carried out without the addition of terminal deoxynucleotidyl transferase.

4.4. Analysis of nuclear morphology

To assess nuclear morphology, cells were stained with 1.0 μM Hoechst 33342 (Molecular Probes [37];) at room temperature for 5 min. Chromatin fluorescence was examined with a Leica inverted fluorescence microscope (Leica Microsystems GmbH) using excitation wavelength of ultraviolet. The cells from six to eight random microscopic fields were counted to calculate the number of stained nuclei. All experiments were repeated at least three times and approximately 300 cells were analyzed per experiment.

4.5. Detection of H_2O_2 and MDA content

The specific fluorescence of H_2O_2 was detected with dichlorodihydrofluorescein diacetate (H_2DCF-DA; Molecular Probes, Eugene, OR) [28,29]. Suspended cells were subjected to $CdCl_2$ (100 μM) or $CdCl_2$ (100 μM) + NaHS (50 μM) for 72 h. Then, cells were fixed on poly-L-lysine-pretreated cover slips (2 × 5 cm) and treated with 50 μM H_2DCF-DA (prepared in LMS) for 5 min at room temperature in the dark. Then the H_2DCF-DA-loaded cells were washed 3–4 times with LMS and analyzed with a Leica inverted fluorescence microscope. The H_2O_2 fluorescence intensity was calculated with Image-Pro Plus 6.0 (Media Cybernetics, Bethesda, MD, USA). MDA content was determined according to the method reported by Li et al. [38].

4.6. Enzyme extraction and activity measurements

Antioxidant enzymes activities were determined according to the method reported by Sun et al. [29]. Collected cell samples (0.2 g) were ground to a fine powder in liquid N_2 and then homogenized in 2 ml of 50 mM potassium phosphate buffer (pH 7.0) containing 1 mM EDTA and 1% polyvinylpyrrolidone (PVP). The homogenate was centrifuged at 10,000 g for 20 min at 4 °C and the supernatant was used to examine antioxidant enzymes, catalase (CAT) and glutathione reductase (GR). For ascorbate peroxidase (APX) measurement, 1 mM ascorbic acid (ASA) was added to the enzyme extraction buffer. Protein concentration was determined, with bovine serum albumin as the standard.

Total CAT activity was determined as the consumption of H_2O_2 (extinction coefficient 39.4 mM^{-1} cm^{-1}) measured at 240 nm for 3 min at 25 °C. The 3 ml reaction mixture contained 50 mM potassium phosphate buffer (pH 7.0), 2% H_2O_2 and 30 μl of cell enzyme extract. Immediately after the enzyme extract was added to the reaction mixture, the initial linear rate of decrease in absorbance at 240 nm was recorded and CAT activity was calculated.

Total GR activity was determined based on the oxidation of NADPH at 340 nm (extinction coefficient 6.2 mM^{-1} cm^{-1}) for 3 min at 25 °C in a 3 ml assay mixture. The mixture contained 50 mM potassium phosphate buffer (pH 7.8), 2 mM EDTA-Na_2, 0.15 mM NADPH, 5 mM GSSG (glutathione disulfide) and 50 μl of cell enzyme extract. The reaction was initiated by the addition of NADPH. Corrections were made for the background absorbance at 340 nm in the absence of NADPH.

Total APX activity was determined as the decrease in A_{290} (extinction coefficient 2.8 mM^{-1} cm^{-1}) for 2 min at 25 °C in a 3 ml

reaction mixture containing 50 mM potassium phosphate buffer (pH 7.0), 15 mM ascorbate, 30 mM H_2O_2 and 30 μl of enzyme extract. The reaction was started by the addition of H_2O_2. Correction was made for the low, non-enzymatic conversion of ascorbate by H_2O_2.

4.7. Visualization of intracellular Cd levels

To evaluate the effects of NaHS on the pattern of intracellular Cd distribution, we used a Cd-specific fluorescent dye, Leadmium™ Green AM, to visualize Cd within cells [5,36]. After $CdCl_2$ (100 μM) and NaHS (50 μM) treatments, suspended cells were loaded with Leadmium™ Green AM (50 μM) for 6 h and analyzed with a Leica SP5 confocal microscopy. The confocal settings were as follows: excitation 488 nm, emission 510–530 nm, frame 512 × 512. The Cd-specific fluorescence in the cytosolic and vacuolar compartments were calculated with Image-Pro Plus 6.0 software (Media Cybernetics, Bethesda, USA).

4.8. Cd flux measurements

Net fluxes of Cd were measured non-invasively using the SIET system (BIO-001A; Younger USA, LLC, MA, USA) [39]. Cd-selective microelectrodes were prepared as described in Sun et al. [39]. The Cd concentration gradients were measured by moving the ion-selective microelectrode between two positions close to the plant material in a preset excursion (10 μm for callus cells and intact vacuoles) at a programmable frequency ranging from 0.3 Hz to 0.5 Hz. The electrode was moved to several positions using a pre-defined sampling routine while being scanned by a three-dimensional microstepper motor manipulator. The ion-selective microelectrode with a 2–4 μm diameter external tip was pre-pulled and silanized with tributylchlorosilane and then backfilled with a commercially available ion-selective cocktail (Cadmium Ionophore I, 20909, Sigma–Aldrich, St Louis, MO, USA). An Ag/AgCl wire electrode holder (XYEH01-1; Xuyue Sci. and Tech. Co., Ltd.) was inserted in the back of the electrode to create an electrical contact with the electrolyte solution. DRIREF-2 (World Precision Instruments) was used as the reference electrode (CMC-4). Prior to the net Cd flux measurements, the microelectrode was calibrated in 5, 10, and 50 μM $CdCl_2$ solution. Only those electrodes with Nernstian slopes that exceed 25 mV/decade were used. The ion flux was calculated using Fick's law of diffusion:

$$J = -D(\mathrm{d}c/\mathrm{d}x),$$

where J represents the ion flux in the x direction, dc/dx is the ion concentration gradient, and D is the ion diffusion constant in a particular medium. The data and image acquisition, preliminary processing, three-dimensional electrode positioner control, and stepper-motor-controlled fine focus of the microscope stage were performed using the ASET software, which is part of the SIET system.

4.8.1. Steady state Cd flux

The *P. euphratica* cells were exposed to $CdCl_2$ (100 μM), $CdCl_2$ + NaHS (50 μM) and $CdCl_2$ + CAT (2000 U ml^{-1}) for 24, 48, 72 h respectively, then immobilized in the measuring solution (10 μM $CdCl_2$, 50 μM $CaCl_2$, pH 5.5) and equilibrated for 15 min [39]. The steady Cd fluxes were then recorded for three to five minutes in each cell. To evaluate the effects of NaHS on the Cd transport across the tonoplast, intact vacuoles were isolated from *P. euphratica* cells for SIET experiments. Firstly, protoplasts were isolated from $CdCl_2$, $CdCl_2$ + NaHS and $CdCl_2$ + CAT-treated *P. euphratica* cells. Cells were incubated in a cell wall-digesting medium consisting of a mannitol medium [700 mM mannitol, 10 mM 2-(*N*-morpholino) ethanesulfonic acid (MES), and 10 μM $CaCl_2$, pH 5.5], 1.5% cellulase Onozuka R-10 (Yakult Honsha), 1% Cellulysin (CalBiochem), and 0.1% pectolyase Y-23 (Yakult Honsha) for 5 h at 28 °C. The released protoplasts were then collected by filtration through a nylon mesh and further purified by gradient centrifugation. Then purified protoplasts were rapidly immersed in a hypoosmotic solution for 3–5 min to release the intact vacuoles. The solution was then replaced by a vacuolar measuring buffer (10 μM $CdCl_2$, 100 mM K-Glu, 700 mM mannitol, 1 μM $CaCl_2$, and 1 mM ATP, pH 7.3). After the vacuoles were fixed on the bottom of the measuring chamber (a 3.5 cm diameter polylysine-pretreated culture dish), the Cd flux across the tonoplast was recorded for three or five minutes in each intact vacuole.

4.8.2. Transient Cd flux across the PM and tonoplast

Control cells or intact vacuoles isolated from control cells were immobilized in the measuring solution (cells: 50 μM $CaCl_2$, pH 5.5, with or without 5 mM $LaCl_3$; vacuoles: 100 mM K-Glu, 700 mM mannitol, 1 μM $CaCl_2$, and 1 mM ATP, pH 7.2 or 5.5). Cd fluxes were continuously recorded for 15 min prior to the addition of $CdCl_2$. Then 10 μM $CdCl_2$ was slowly added to the solution by a pipettor and Cd flux was recorded for 15 min. Afterwards, 3 mM H_2O_2 was slowly added to the solution and the Cd flux were recorded for 15 min. The Cd fluxes were calculated using MageFlux, which was developed by the Xu-Yue company (http://xuyue.net/mageflux).

4.9. Data analysis

All mean data were subjected to analysis of variance. Significant differences between means were determined by Duncan's multiple range test. Unless otherwise stated, differences were considered statistically significant when $P < 0.05$.

Acknowledgements

This work was financially supported jointly by the National Science Foundation of China (Nos. 31200470, 31270654, 31170570, 31271698, 31200207), the Scientific Research Support Project for Teachers with Doctor's Degrees (Jiangsu Normal University, China, No. 11XLR23), the Priority Academic Program Development of Jiangsu Higher Education Institutions (PAPD), the Natural Science Fund for Colleges and Universities in Jiangsu Province (No. 12KJB180003), Beijing Natural Science Foundation (No. 6112017), and the Program of Introducing Talents of Discipline to Universities (111 Project, No. B13007).

References

[1] A. Schützendübel, A. Polle, Plant responses to abiotic stresses: heavy metal-induced oxidative stress and protection by mycorrhization, J. Exp. Bot. 53 (2002) 1351–1365.
[2] A. Lux, M. Martinka, M. Vaculik, P.J. White, Root responses to cadmium in the rhizosphere: a review, J. Exp. Bot. 62 (2011) 21–37.
[3] G. DalCorso, S. Farinati, S. Maistri, A. Furini, How plants cope with cadmium: staking all on metabolism and gene expression, J. Integr. Plant Biol. 50 (2008) 1268–1280.
[4] S.M. Gallego, L.B. Pena, R.A. Barcia, C.E. Azpilicueta, M.F. Iannone, E.P. Rosales, M.S. Zawoznik, M.D. Groppa, M.P. Benavides, Unravelling cadmium toxicity and tolerance in plants: insight into regulatory mechanisms, Environ. Exp. Bot. 83 (2012) 33–46.
[5] S. Tian, L. Lu, J. Labavitch, X. Yang, Z. He, H. Hu, R. Sarangi, M. Newville, J. Commisso, P. Brown, Cellular sequestration of cadmium in the hyperaccumulator plant species *Sedum alfredii*, Plant Physiol. 157 (2011) 1914–1925.
[6] U. Kramer, Metal hyperaccumulation in plants, Annu. Rev. Plant Biol. 61 (2010) 517–534.
[7] N. Verbruggen, C. Hermans, H. Schat, Mechanisms to cope with arsenic or cadmium excess in plants, Curr. Opin. Plant Biol. 12 (2009) 364–372.

[8] V. Korenkov, K. Hirschi, J.D. Crutchfield, G.J. Wagner, Enhancing tonoplast Cd/H antiport activity increases Cd, Zn, and Mn tolerance, and impacts root/shoot Cd partitioning in *Nicotiana tabacum L*, Planta 226 (2007) 1379–1387.
[9] V. Korenkov, B. King, K. Hirschi, G.J. Wagner, Root-selective expression of *AtCAX4* and *AtCAX2* results in reduced lamina cadmium in field-grown *Nicotiana tabacum L*, Plant Biotechnol. J. 7 (2009) 219–226.
[10] M. Morel, J. Crouzet, A. Gravot, P. Auroy, N. Leonhardt, A. Vavasseur, P. Richaud, AtHMA3, a P_{1B}-ATPase allowing Cd/Zn/Co/Pb vacuolar storage in Arabidopsis, Plant Physiol. 149 (2009) 894–904.
[11] G. Tanou, V. Fotopoulos, A. Molassiotis, Priming against environmental challenges and proteomics in plants: update and agricultural perspectives, Front. Plant Sci. 3 (2012) 216.
[12] M. Hasanuzzaman, M.A. Hossain, M. Fujita, Exogenous selenium pretreatment protects rapeseed seedlings from cadmium-induced oxidative stress by upregulating antioxidant defense and methylglyoxal detoxification systems, Biol. Trace Elem. Res. 149 (2012) 248–261.
[13] M.M. Islam, M.A. Hoque, E. Okuma, M.N. Banu, Y. Shimoishi, Y. Nakamura, Y. Murata, Exogenous proline and glycinebetaine increase antioxidant enzyme activities and confer tolerance to cadmium stress in cultured tobacco cells, J. Plant Physiol. 166 (2009) 1587–1597.
[14] J. Xiong, L. An, H. Lu, C. Zhu, Exogenous nitric oxide enhances cadmium tolerance of rice by increasing pectin and hemicellulose contents in root cell wall, Planta 230 (2009) 755–765.
[15] L. Lu, S. Tian, M. Zhang, J. Zhang, X. Yang, H. Jiang, The role of Ca pathway in Cd uptake and translocation by the hyperaccumulator *Sedum alfredii*, J. Hazard. Mater. 183 (2010) 22–28.
[16] A. Masood, N. Iqbal, N.A. Khan, Role of ethylene in alleviation of cadmium-induced photosynthetic capacity inhibition by sulphur in mustard, Plant Cell Environ. 35 (2012) 524–533.
[17] L. Li, P. Rose, P.K. Moore, Hydrogen sulfide and cell signaling, Annu. Rev. Pharmacol. Toxicol. 51 (2011) 169–187.
[18] Y.T. Lin, M.Y. Li, W.T. Cui, W. Lu, W.B. Shen, Haem oxygenase-1 is involved in hydrogen sulfide-induced cucumber adventitious root formation, J. Plant Growth Regul. 31 (2012) 519–528.
[19] M. Lisjak, N. Srivastava, T. Teklic, L. Civale, K. Lewandowski, I. Wilson, M.E. Wood, M. Whiteman, J.T. Hancock, A novel hydrogen sulfide donor causes stomatal opening and reduces nitric oxide accumulation, Plant Physiol. Biochem. 48 (2010) 931–935.
[20] J. Chen, F.H. Wu, W.H. Wang, C.J. Zheng, G.H. Lin, X.J. Dong, J.X. He, Z.M. Pei, H.L. Zheng, Hydrogen sulfide enhances photosynthesis through promoting chloroplast biogenesis, photosynthetic enzyme expression, and thiol redox modification in *Spinacia oleracea* seedlings, J. Exp. Bot. 62 (2011) 4481–4493.
[21] Z. Jin, J. Shen, Z. Qiao, G. Yang, R. Wang, Y. Pei, Hydrogen sulfide improves drought resistance in *Arabidopsis thaliana*, Biochem. Biophys. Res. Commun. 414 (2011) 481–486.
[22] Y.Q. Wang, L. Li, W.T. Cui, S. Xu, W.B. Shen, R. Wang, Hydrogen sulfide enhances alfalfa (*Medicago sativa*) tolerance against salinity during seed germination by nitric oxide pathway, Plant Soil 351 (2012) 107–119.
[23] H. Zhang, Z.Q. Tan, L.Y. Hu, S.H. Wang, J.P. Luo, R.L. Jones, Hydrogen sulfide alleviates aluminum toxicity in germinating wheat seedlings, J. Integr. Plant Biol. 52 (2010) 556–567.
[24] L. Li, Y. Wang, W. Shen, Roles of hydrogen sulfide and nitric oxide in the alleviation of cadmium-induced oxidative damage in alfalfa seedling roots, Biometals 25 (2012) 617–631.
[25] A. Polle, C. Douglas, The molecular physiology of poplars: paving the way for knowledge-based biomass production, Plant Biol. 12 (2010) 239–241.
[26] S. Castiglione, V. Todeschini, C. Franchin, P. Torrigiani, D. Gastaldi, A. Cicatelli, C. Rinaudo, G. Berta, S. Biondi, G. Lingua, Clonal differences in survival capacity, copper and zinc accumulation, and correlation with leaf polyamine levels in poplar: a large-scale field trial on heavily polluted soil, Environ. Pollut. 157 (2009) 2108–2117.
[27] J. Sun, S. Chen, S. Dai, R. Wang, N. Li, X. Shen, X. Zhou, C. Lu, X. Zheng, Z. Hu, Z. Zhang, J. Song, Y. Xu, NaCl-induced alternations of cellular and tissue ion fluxes in roots of salt-resistant and salt-sensitive poplar species, Plant Physiol. 149 (2009) 1141–1153.
[28] J. Sun, M. Wang, M. Ding, S. Deng, M. Liu, C. Lu, X. Zhou, X. Shen, X. Zheng, Z. Zhang, J. Song, Z. Hu, Y. Xu, S. Chen, H_2O_2 and cytosolic Ca^{2+} signals triggered by the PM H^+-coupled transport system mediate K^+/Na^+ homeostasis in NaCl-stressed *Populus euphratica* cells, Plant Cell Environ. 33 (2010) 943–958.
[29] J. Sun, L. Li, M. Liu, M. Wang, M. Ding, S. Deng, C. Lu, X. Zhou, X. Shen, X. Zheng, S. Chen, Hydrogen peroxide and nitric oxide mediate K^+/Na^+ homeostasis and antioxidant defense in NaCl-stressed callus cells of two contrasting poplars, Plant Cell, Tissue Organ Cult. 103 (2010) 205–215.
[30] S. Chen, A. Polle, Salt tolerance in *Populus*, Plant Biol. 12 (2010) 317–333.
[31] J. Sun, S. Dai, R. Wang, S. Chen, N. Li, X. Zhou, C. Lu, X. Shen, X. Zheng, Z. Hu, Z. Zhang, J. Song, Y. Xu, Calcium mediates root K^+/Na^+ homeostasis in poplar species differing in salt tolerance, Tree Physiol. 29 (2009) 1175–1186.
[32] A. Polle, T. Klein, C. Kettner, Impact of cadmium on young plants of *Populus euphratica* and *P.× canescens*, two poplar species that differ in stress tolerance, New For. 44 (2013) 13–22.
[33] R. De Michele, E. Vurro, C. Rigo, A. Costa, L. Elviri, M. Di Valentin, M. Careri, M. Zottini, L.S. di Toppi, F. Lo Schiavo, Nitric oxide is involved in cadmium-induced programmed cell death in Arabidopsis suspension cultures, Plant Physiol. 150 (2009) 217–228.
[34] L. Perfus-Barbeoch, N. Leonhardt, A. Vavaddeur, C. Forestier, Heavy metal toxicity: cadmium permeates through calcium channels and disturbs the plant water status, Plant J. 32 (2002) 539–548.
[35] V. Demidchik, S. Shabala, J. Davies, Spatial variation in H_2O_2 response of *Arabidopsis thaliana* root epidermal Ca^{2+} flux and plasma membrane Ca^{2+} channels, Plant J. 49 (2007) 377–386.
[36] J. Park, W. Song, D. Ko, Y. Eom, T.H. Hansen, M. Schiller, T.G. Lee, E. Martinoia, Y. Lee, The phytochelatin transporters AtABCC1 and AtABCC2 mediate tolerance to cadmium and mercury, Plant J. 69 (2012) 278–288.
[37] J. Sun, C.L. Zhang, S.R. Deng, C.F. Lu, X. Shen, X.Y. Zhou, X.J. Zheng, Z.M. Hu, S.L. Chen, An ATP signalling pathway in plant cells: extracellular ATP triggers programmed cell death in *Populus euphratica*, Plant Cell Environ. 35 (2012) 893–916.
[38] Z. Li, M. Gong, H. Xie, L. Yang, J. Li, Hydrogen sulfide donor sodium hydrosulfide-induced heat tolerance in tobacco (*Nicotiana tabacum L*) suspension cultured cells and involvement of Ca^{2+} and calmodulin, Plant Sci. 186 (2012) 185–189.
[39] J. Sun, R. Wang, Z. Liu, Y. Ding, T. Li, Non-invasive microelectrode cadmium flux measurements reveal the spatial characteristics and real-time kinetics of cadmium transport in hyperaccumulator and nonhyperaccumulator ecotypes of *Sedum alfredii*, J. Plant Physiol. 170 (2013) 355–359.